Photoelectron Spectroscopic Investigation of Nitrogen-Doped Titania Nanoparticles

Xiaobo Chen and Clemens Burda*

Center for Chemical Dynamics and Nanomaterials Research, Department of Chemistry, Case Western Reserve University, 10900 Euclid Avenue, Cleveland, Ohio 44106-7078

Received: July 12, 2004; In Final Form: August 26, 2004

A series of titania (TiO_2)-based nanometer-sized photocatalysts, including nitrogen-doped TiO_2 nanoparticles (NPs), are investigated using X-ray photoelectron spectroscopy (XPS). Conclusive evidence is obtained for O−Ti−N bond formation during the doping process. Therefore, this substitutional doping is held accountable for the significant increase in photocatalytic activity in nitrogen-doped TiO_2 NPs.

Nanomaterials have attracted much attention over the past decade, because of their unique properties, which include quantum confinement and a heightened reactivity associated with changes in their molecular electronic structure and/or an increase in surface-to-volume ratio.[1−4] Particularly, titanium dioxide (TiO_2) nanoparticles (NPs) have gained great interest, because of their potential as photovoltaics, photochromic sensors, and photocatalysts.[5−7] Highly efficient usage of TiO_2 in photocatalysis applications is prevented by its wide band gap (3.2 eV), which responds to only a small fraction of the sun's energy spectrum. Therefore, one of the endeavors to improve the performance of TiO_2 is to increase its optical activity by shifting the onset of its response from the ultraviolet (UV) to the visible region.[8−10]

Enhanced photocatalytic activity has been reported for metal-doped TiO_2 at a doping of 0.5%.[5] However, studies also reveal that metal doping can result in thermal instability and increased carrier trapping.[11,12] The visible-light response for nitrogen-doped TiO_2 was first discovered by Sato, where an NO_x impurity was attributed for the sensitization of the visible light.[8] Moreover, recent theoretical and experimental studies have shown that the desired band gap narrowing of TiO_2 can be achieved using main-group dopants, to enhance the photoactivity of TiO_2 in the visible spectral range.[9,10,13,14] It was predicted by theory and demonstrated in experiments[9] that nitrogen-doped TiO_2 films exhibit improved catalysis under visible-light excitation. Recently, we reported the formation and highly photocatalytic activity of $TiO_{2-x}N_x$ NPs.[10] However, the actual formation of O−Ti−N domains in the lattice of the host NPs has not yet been demonstrated, and, therefore, structural evidence for the formation of substitutional O−Ti−N sites within the nitrogen-doped TiO_2 NPs still remains elusive to date.

Here, we report an extended X-ray photoelectron spectroscopy (XPS) analysis of nitrogen incorporation in TiO_2 nanostructured materials. The synthesized nitrogen-doped NPs are compared to a series of titania-based nanomaterials, which includes the commercially available TiO_2 Degussa P25 nanopowder.[10,15] The experimental evidence suggests O−Ti−N bond formation during the doping process, which accounts for the significant increase in photocatalytic activity in the nitrogen-doped titania NPs.

The inset in Figure 1A shows a transmission electron microscopy (TEM) image of the doped TiO_2 NPs, with an average diameter of ∼10 nm, which also is confirmed with the XRD measurement.[10] Global XPS profiles for the titania and nitrided titania samples are shown in Figure 1A. The XPS technique monitors the electron binding energy of sites within a few nanometers of the particle surfaces. Recently, a study has been performed using depth profiling on combined titanium oxide−titanium nitride (TiO_2−TiN) systems,[16] which is the subject of the current study. The authors determined the chemical composition of the TiN layer on the top surface using XPS, as well as after Ar^+ ion sputtering. They reported the formation of Ti−N and Ti−O bonds and concluded a Ti−N−O formation.[16] From our measurements, we find that a nitrogen content of 4%−8% is incorporated into the lattice of the synthesized TiO_2 NPs. In comparison, a nitrogen content of <1% can be detected in the amine-treated P25 sample. The synthesized nanometer-sized TiO_2 particles seem to be more receptive for nitrogen uptake (sensitivity factors for Ti, N, and O were taken into account). Figure 1B shows the N 1s peak for these samples.

For further analysis of the chemical structure of the investigated TiO_2 samples, we have examined three areas of the XPS spectrum: the N 1s region near 400 eV (Figure 1B), the Ti 2p region near 460 eV (Figure 2), and the O 1s region near 530 eV (Figure 3). In these three regions, there are distinct differences between the synthesized NPs and the commercially available P25 samples. The binding energy peak of N 1s for the nitrogen-doped TiO_2 NPs is broad, extending from 397.4 eV to 403.7 eV. It is centered at 401.3 eV, which is a value that is greater than the typical binding energy of 397.2 eV in TiN[17] and, therefore, can be attributed to the 1s electron binding energy of the N atom in the environment of O−Ti−N. This shift in binding energy can be understood by the fact that the N 1s electron binding energy is higher when the formal charge of N is more positive (e.g., 408 eV in $NaNO_3$), compared to zero or a negative formal charge (398.8 eV in NH_3).[18] The local electron density around N is lower for more-positive formal charges. When nitrogen substitutes for the oxygen in the initial O−Ti−O structure, the electron density around N is reduced, compared to that in a TiN crystal, because of the O atom on the Ti atom. Thus, the N 1s binding energy in an O−Ti−N environment is higher than that in an N−Ti−N environment where the N atom replaces the O atom.

When scanning the Ti 2p and O 1s XPS regions, major differences for the original binding energies and their nitrogen-treated counterparts are noted. First, for the Ti 2p (Figure 2A),

* Author to whom correspondence should be addressed. E-mail address: burda@cwru.edu.

10.1021/jp0469160 CCC: $27.50
Published on Web 09/15/2004

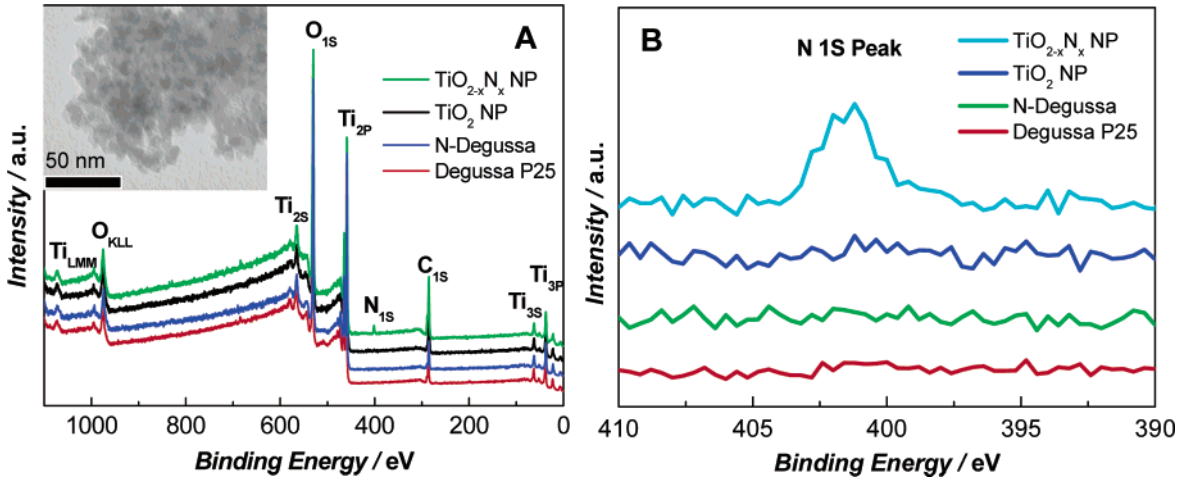

Figure 1. **(**A**)** Comparison of the X-ray photoelectron spectra of P25 TiO_2 powder (red), nitrided P25 TiO_2 powder (blue), TiO_2 nanoparticles (NPs) (black), and $TiO_{2-x}N_x$ NPs (green). Inset shows the TEM image for the $TiO_{2-x}N_x$ NPs. **(**B**)** The N 1s peak of these samples around the 400 eV region.

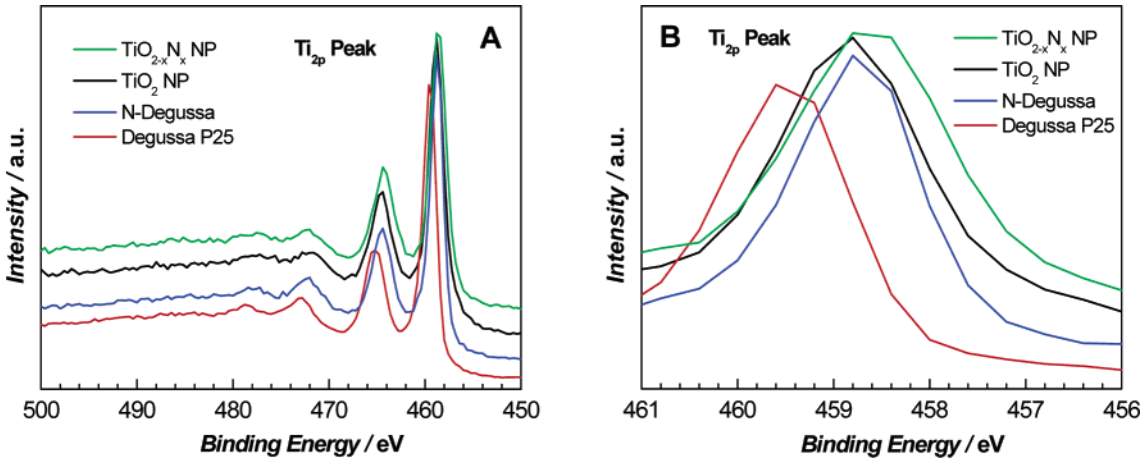

Figure 2. **(**A**)** The Ti 2p peak at ~460 eV of P25 TiO_2 powder (red), nitrided P25 TiO_2 powder (blue), TiO_2 NPs (black), and nitrided $TiO_{2-x}N_x$ NPs (green). **(**B**)** The Ti $2p_{3/2}$ peak of these samples around the 460 eV region.

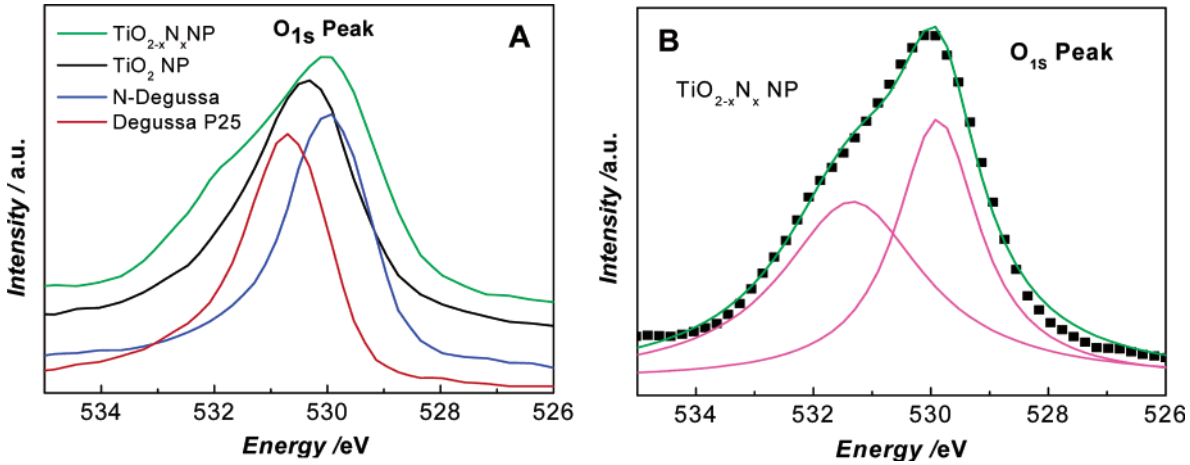

Figure 3. **(**A**)** The O 1s peak at ~460 eV of P25 TiO_2 powder (red), nitrided P25 TiO_2 powder (blue), TiO_2 NP particles (black), and $TiO_{2-x}N_x$ NP (green). **(**B**)** For the nitrided NP, the O 1s peak displays a second signal that is shifted to higher binding energy, because of the formation of a O−Ti−N bond.

especially the Ti $2p_{3/2}$ region, depicted in Figure 2B, one observes a peak close to 459.7 eV for the P25 powder, located at notably higher binding energy than that for the remaining samples. In comparison, the corresponding peak of the synthesized NPs appears at 458.8 eV, which is a notably lower binding energy. The shift in the XPS signals with nitrogen incorporation in the 10-nm NP sample is toward the lowest binding energy. As discussed previously, a shift toward lower binding energy upon nitrogen treatment displays the successful incorporation of nitrogen into the TiO_2 lattice.[17] The treated P25 sample shows a peak at 459.7 eV and the nitrided NPs at 458.8 eV. This is significantly lower (0.9 eV) in binding energy, indicating the highest nitrogen incorporation in the synthesized TiO_2 NPs. The typical binding energy of the Ti $2p_{3/2}$ peak in TiO_2 crystals is

458.5−459.7 eV, which is higher than that in TiN crystals (455.1 eV).[18−22]

After doping (when the N atom replaces the O atom out of the lattice), the valence state of the Ti cation can be reduced. The binding energy of the Ti $2p_{3/2}$ peak shifts to lower energies when the valence state of Ti^{4+} is reduced to Ti^{3+} and Ti^{2+}.[19] This is also true for TiO, TiS, TiN, and TiP compounds, where the valence states of Ti are Ti^{2+} and Ti^{3+}.[23] Thus, the observed Ti $2p_{3/2}$ binding energy after nitrogen treatment can be attributed to the formation of O−Ti−N bonding by partially substituting the O atom in the TiO_2 lattice with a N atom. This shifts the binding energies of the Ti 2p electrons to the observed lower values.

The observed XPS peaks for the Ti 2p region, and their change relative to nitrogen incorporation, are strikingly consistent with the recent XPS depth profiling characterization of Gyorgy et al.[16] These authors also observed a shift in the Ti 2p binding energy to lower energies as the TiO_2 surface was nitrided. Furthermore, the observations in the present study are consistent with the earlier results of Saha and Tomkins,[17] who have used XPS to characterize the oxidation of a TiN surface—in essence, the reverse of the current experiment and that of Gyorgy et al.[16]

The O 1s XPS spectra in Figure 3A also show significant changes upon nitrogen incorporation, the most significant being an additional signal at higher binding energy than the main oxygen feature for the prepared NPs. In Figure 3, the P25 sample shows an O 1s peak at 530.8 eV, versus a shift to ∼530.0 eV that is observed for both the nitrogen-doped P25 and NP samples.

As shown in Figure 3B, an additional peak in the $TiO_{2-x}N_x$ NPs appears at 532 eV. It is a feature that was first observed by Saha and Tomkins[17] and was most recently characterized by Gyorgy et al.[16] in their depth profiling study on TiN surfaces. Gyorgy et al. assigned this feature to the formation of oxidized Ti−N, which leads to the Ti−O−N structure.[16] Our study suggests that the appearance of this peak is a consistent feature for the nitrogen substitution in TiO_2 and signifies the formation of an O−Ti−N structure.

In analogy to the classic paper of Saha and Tomkins,[17] we suggest that the Ti $2p_{3/2}$ XPS peak at 459.5 eV is consistent with the formation of a crystalline TiO_2 sample. The nitrogen incorporation shifts the XPS spectrum to a lower binding energy (a peak is observed at ∼458.8 eV). The final binding energies are higher for the doped P25 TiO_2 NPs. Because of surface strain and lattice distortion, which are available in the synthesized TiO_2 NP lattice,[10,24,25] one would expect that the incorporation of the amine and its subsequent reaction to occur more readily in the prepared NPs. The smaller NPs seem to take up the nitrogen much easier, possibly because of larger lattice strain, and the larger P25 do not proceed as readily, because the surface is already relaxed and any doping poses a steric problem, which is also suggested by the significant shifts in the XPS binding energies. Therefore, it is not surprising that one observes a much higher binding energy of the XPS Ti 2p and O 1s peaks in the P25 sample, compared to the TiO_2 NPs. The structure of the P25 sample is such that the nitrogen perturbs the TiO_2 lattice and changes the Ti−O bond, shifting the infrared transitions to higher energy. In the TiO_2 NP, the nitrogen could have a very different effect on the Ti−O bond, because these structures are already considerably more-strained.[24,25] The nitrogen, which is incorporated to form the O−Ti−N structure, is observed to shift the O−Ti−O infrared feature to higher frequencies. Thus, the observed changes in the XPS spectra are providing consistent structural information for O−Ti−N formation, the substitutional doping of nitrogen for oxygen, which leads to the enhanced photocatalytic activity observed in ∼10-nm nitrogen-doped NPs.

In addition, Rodriguez et al. recently measured the XPS spectra of NO, NO_2, and NO_3 on a ZnO surface.[26] This allowed us to confirm, for our study, that no such nitrogen oxide species are formed on the NP surface. Although the N 1s peaks for NO and NO_2 are detected (at 400 and 405 eV, respectively), our N 1s signal was observed at 402 eV. This is again additional evidence for the O−Ti−N structure. Moreover, Rodriguez et al. measured the O 1s peak for −NO and $-NO_2$ at 533.5 eV,[26] compared to the 532 eV value in our study. Therefore, we can exclude that the novel properties would be related to surface-oxidized nitrogen species.

The active site and the nitrogen state responsible for the enhanced photocatalytic activity of nitrogen-doped TiO_2 is a recent subject of photocatalytic research.[9,10] Asahi reported that substitutional nitrogen was responsible for the enhanced activity both from their calculation and experiments.[9] They further correlated it to the nitrogen XPS peak intensity at 396 eV, and from the correlation to the photocatalytic activity, they obtained an optimum nitrogen concentration in nitrogen-doped TiO_2 films.[9] Following Asahi, there were several reports on the nitrogen, appearing in the XPS spectrum at 396 eV, and related enhanced photocatalytic activity.[27−30] A linear increase of the visible-light response to the XPS intensity of the nitrogen at 396 eV was reported recently in nitrogen-doped nanopowders.[27] However, the signal-to-noise ratio for the N 1s XPS analysis was rather low. Recently, Diwald et al. studied nitrogen-doped TiO_2 and their photoactivities for rutile single crystals.[29,30] In one case, where the doped TiO_2 sample was prepared by sputtering TiO_2 with a N^{2+}/Ar^+ gas mixture, followed by annealing, the N peak at 396 eV was observed and attributed to a chemically bound N^- species within the crystalline TiO_2 lattice.[29] In another study,[30] where a doped TiO_2 sample was prepared by treating TiO_2 with NH_3 flow at high temperature, the enhanced photocatalytic activity was attributed to the nitrogen with a binding energy of 399.6 eV, although a N peak at 396 eV was detected. The photocatalytically active N site was attributed to chemically bound hydrogen and interstitial doping into the TiO_2 lattice.[30]

However, the N peak at 396 eV was not always observed.[31] In the recent report on nitrogen-doped titania by Sakthivel, a nitrogen peak around 404 eV was observed, while the signal at 396 eV was completely absent.[31] Thus, the nitrogen state in the doped TiO_2 may vary from case to case. For the currently presented nanoparticles, the signal at 401.3 eV is attributed to O−Ti−N, based on the redox chemistry involved and the XPS peak positions of oxygen, titanium, and nitrogen itself.

In conclusion, global and detailed XPS analyses are applied to a series of titania (TiO_2)-based nanomaterials, which includes nitrogen-doped TiO_2 nanoparticles (NPs) and Degussa P25 powder. The formation of a O−Ti−N structure is suggested as the chemical structure formed during the substitutional doping process, and it is attributed to be responsible for the significant increase in photocatalytic activity that has been previously observed for synthesized nitrogen-doped NPs.

Acknowledgment. C.B. gratefully acknowledges financial support from NSF Grant (No. CHE-0239688) and ACS-PRF (No. 39881-G5M). We gratefully acknowledge Dr. W. Jennings for the support for XPS measurements and Prof. J. Gole for fruitful discussions.

References and Notes

(1) Alivisatos, A. P. *J. Phys. Chem.* **1996**, *100*, 13226.
(2) Nirmal, M.; Brus, L. *Acc. Chem. Res.* **1999**, *32*, 407.
(3) Murray, C. B.; Kagan, C. R.; Bawendi, M. G. *Annu. Rev. Mater. Sci.* **2000**, *30*, 545.
(4) Burda, C.; El-Sayed, M. A. *Pure Appl. Chem.* **2000**, *72*, 165.
(5) Hoffmann, M. R.; Martin, S. T.; Choi, W.; Bahnemann, D. W. *Chem. Rev.* **1995**, *95*, 69.
(6) Grätzel, M. *Nature* **2001**, *414*, 338.
(7) Millis, A.; Hunte, S. L. *J. Photochem. Photobiol. A* **1997**, *108*, 1.
(8) Sato, S. *Chem. Phys. Lett.* **1986**, *123*, 126.
(9) Asahi, R.; Morikawa, T.; Ohwaki, T.; Aoki, K.; Taga, Y. *Science* **2001**, *293*, 269.
(10) (a) Burda, C.; Lou, Y.; Chen, X.; Samia, A. C. S.; Stout, J.; Gole, J. L. *Nano Lett.* **2003**, *3*, 1049. (b) Gole, J. L.; Stout, J.; Burda, C.; Lou, Y.; Chen, X. *J. Phys. Chem. B* **2004**, *108*, 1230.
(11) Yamashita, H.; Honda, M.; Harada, M.; Ichihashi, Y.; Anpo, M.; Hirao, T.; Itoh, N.; Iwamoto, N. *J. Phys. Chem. B* **1998**, *102*, 10707.
(12) Wang, Y.; Cheng, H.; Hao, Y.; Ma, J.; Li, W.; Cai, S. *Thin Solid Films* **1999**, *349*, 120.
(13) Yu, J. C.; Yu, J. G.; Ho, W. K.; Jiang, Z. T.; Zhang, L. Z. *Chem. Mater.* **2002**, *14*, 3808.
(14) Khan, S. U. M.; Al-Shahry, M., Jr.; Ingler, W. B. *Science* **2002**, *297*, 2243.
(15) The TiO_2 nanocrystals are prepared via the hydrolysis of $Ti[OCH(CH_3)_2]_4$ (dissolved in isopropyl alcohol) in water with a pH of 2.0. Treatment of the initial nanoparticle solution with an excess of triethylamine results in the formation of the nitrided TiO_2 nanoparticles. The nitrided Degussa sample was obtained by reacting ~0.5 g of Degussa with 10 mL of triethylamine for >4 h at 80 °C. Upon vacuum drying (5×10^{-2} Torr) for several hours, this treatment resulted in the isolation of yellow-brown crystallites. The X-ray diffraction (XRD) patterns were obtained using a Philips model PW 3710 powder X-ray diffractometer. The transmission electron microscopy (TEM) images were obtained on a Philips model CM20 transmission electron microscope. The XPS spectra were measured on a Perkin−Elmer model PHI 5600 XPS system with a resolution of 0.3−0.5 eV from a monochromated aluminum anode X-ray source with Kα radiation (1486.6 eV). The samples were coated on the carbon tape that was attached to the sample holder. The binding energies of the Ti 2p, N 1s, and O 1s peaks from the samples were calibrated, with respect to the C 1s peak, from the carbon tape at 284.6 eV.
(16) Gyorgy, E.; Perez del Pino, A.; Serra, P.; Morenza, J. L. *Surf. Coat. Technol.* **2003**, *173*, 265.
(17) Saha, N. C.; Tomkins, H. C. *J. Appl. Phys.* **1992**, *72*, 3072.
(18) NIST/EPA Gas-Phase Infrared Database, http://webbook.nist.gov/chemistry/; http://srdata.nist.gov/xps/.
(19) Hashimoto, S.; Murata, A.; Sakurada, T.; Tanaka, A. *J. Surf. Anal.* **2002**, *9*, 459.
(20) Yoshitake, M.; Thananan, A.; Aizawaki, T.; Yoshihara, K. *Surf. Interface Anal.* **2002**, *34*, 698.
(21) Wang, Y. L. *Surf. Coat. Technol.* **2002**, *150*, 257.
(22) Gall, D.; Haasch, R. T.; Finnegan, N.; et al. *Surf. Sci. Spectra* **2000**, *7*, 167.
(23) Berger, H.; Tang, H.; Lévy, F. *J. Cryst. Growth* **1993**, *130*, 108.
(24) Chen, X.; Lou, Y.; Samia, A. C.; Burda, C. *Nano Lett.* **2003**, *3*, 799.
(25) Zhang, X.; Wang, M. X.; Qu, L.; Peng, X. *Appl. Phys. Lett.* **2002**, *81*, 2076.
(26) Rodriguez, J. A.; Jirsak, T.; Dvorak, J.; Sambasivan, S.; Fischer, D. *J. Phys. Chem. B* **2000**, *104*, 319.
(27) Irie, H.; Watanabe, Y.; Hashimoto, K. *J. Phys. Chem. B* **2003**, *107*, 5483.
(28) Sano, T.; Negishi, N.; Koike, K.; Takeuchi, K.; Matsuzawa, S. *J. Mater. Chem.* **2004**, *14*, 380.
(29) Diwald, O.; Thompson, T. L.; Goralski, E. G.; Walck, S. D.; Yates, J. T., Jr. *J. Phys. Chem. B* **2004**, *108*, 52.
(30) Diwald, O.; Thompson, T. L.; Zubkov, T.; Goralski, E. G.; Walck, S. D.; Yates, J. T., Jr. *J. Phys. Chem. B* **2004**, *108*, 52.
(31) Sakthivel, S.; Kisch, H. *ChemPhysChem* **2003**, *4*, 487.